

**COSMIC RAYS IN THE ENERGY RANGE OF THE KNEE
– RECENT RESULTS FROM KASCADE –**

K.-H. KAMPERT^{1,2*}, T. ANTONI², W.D. APEL², F. BADEA³, K. BEKK²,
K. BERNLÖHR², H. BLÜMER^{2,1}, E. BOLLMANN², H. BOZDOG³,
I.M. BRANCUS³, C. BÜTTNER², A. CHILINGARIAN⁴, K. DAUMILLER¹,
P. DOLL², J. ENGLER², F. FEßLER², H.J. GILS², R. GLASSTETTER¹,
R. HAEUSLER², A. HAUNGS², D. HECK², T. HOLST², J.R. HÖRANDEL¹,
A. IWAN⁵, J. KEMPA⁵, H.O. KLAGES², J. KNAPP¹, G. MAIER²,
H.-J. MATHES², H.J. MAYER², J. MILKE², M. MÜLLER²,
J. OEHLISCHLÄGER², M. PETCU³, H. REBEL², M. RISSE², M. ROTH²,
G. SCHATZ², H. SCHIELER², J. SCHOLZ², T. THOUW², H. ULRICH¹,
B. VULPESCU³, J.H. WEBER¹, J. WENTZ², J. WOCHLE²,
J. ZABIEROWSKI⁶, S. ZAGROMSKI²

¹ *Institut für Exp. Kernphysik, Universität Karlsruhe (TH), (Germany)*

² *Institut für Kernphysik, Forschungszentrum Karlsruhe, (Germany)*

³ *Institute of Physics and Nuclear Engineering, Bucharest, (Romania)*

⁴ *Cosmic Ray Division, Yerevan Physics Institute, (Armenia)*

⁵ *Department of Experimental Physics, University of Lodz, (Poland)*

⁶ *Institute for Nuclear Studies, Lodz, (Poland)*

A brief motivation for studying cosmic rays at energies $10^{14} \lesssim E \lesssim 10^{17}$ eV is given. Besides astrophysical interests in identifying and understanding their sources, there are also particle physics aspects related to their transport properties in the galaxy or to their detection via extensive air showers. The KASCADE air shower experiment taking data at Forschungszentrum Karlsruhe (Germany) provides important information to both of these topics of particle-astrophysics research. A target of particular interest is the so-called “knee” in the cosmic ray energy spectrum at $E_k \approx 4 \cdot 10^{15}$ eV. Recent results adding knowledge to an understanding its origin will be presented as well as results on tests of high-energy hadronic interaction models required for air shower simulations.

1 Introduction

The origin and acceleration mechanism of ultra-high energy cosmic rays have been subject to debate for several decades. Mainly for reasons of the power required to maintain the observed cosmic ray energy density of $\varepsilon_{\text{cr}} \approx 1 \text{ eV/cm}^3$ the dominant acceleration sites are generally believed to be supernova remnants (SNR). Charged particles mainly originating from the surrounding interstellar medium of the pre-supernova star may get trapped at the highly

*E-MAIL: KAMPERT@IK1.FZK.DE

supersonic shock wave generated by the SN explosion. Repeatedly reflections on both sides of the shock front lead to an acceleration by the so-called ‘first order Fermi mechanism’. Naturally, this leads to a power law spectrum $dj/dE \propto E^{-\gamma}$ as is observed experimentally. Simple dimensional estimates show that this process is limited to $E_{\max} \lesssim Z \times (\rho \times B)$, with Z being the atomic number of the cosmic ray (CR) isotope and ρ , B the size and magnetic field strength of the acceleration region. A more detailed examination of the astrophysical parameters suggests an upper limit of acceleration of $E_{\max} \approx Z \times 10^{15} \text{ eV}^{1,2}$. Curiously, the CR spectrum steepens from $\gamma \simeq 2.75$ to $\simeq 3.1$ at $E \simeq 4 \times 10^{15} \text{ eV}$ which is called the ‘knee’. The coincidence thus may indicate that the ‘knee’ is related to the upper limit of acceleration.

An alternative interpretation of the knee is that it may reflect a change in the propagation of CRs from their sources to the solar system. Propagation effects are studied mostly by balloon or space borne experiments measuring abundances of secondary to primary CR isotopes at energies up to some GeV. A prominent example is the B/C-ratio. Analysing such data yields the ‘escape time’ of CRs from our galaxy which scales with energy according to $\tau_{\text{esc}} \propto E^{-\delta}$ with $\delta \approx 0.6$. A simple extrapolation of τ_{esc} to higher energies breaks down at $E \approx 3 \cdot 10^{15} \text{ eV}$, because $c\tau_{\text{esc}} \sim 300 \text{ pc}$ which is the thickness of the galactic disk³. The value corresponds to just one crossing of the disk and would give rise to significant anisotropies with respect to the galactic plane when approaching this value. Similarly as to the process of acceleration at SNR shocks, the process of galactic containment is closely related to magnetic field confinement, i.e. in addition to anisotropies one again expects $E_{\max}^{\text{gal}} \propto Z$.

A picture related to both of these interpretations has been proposed by Erlykin and Wolfendale⁴. They consider the knee as a superposition of a weakly energy dependent galactic modulation with additional prominent structures in the flux spectrum caused by a single near-by object. This so-called ‘single source model’ assumes that a shock wave of a recent nearby supernova which exploded some 10,000 years ago at a distance of a few hundred parsecs currently propagates, or has recently propagated through the solar system causing distinct peaks of elemental groups in the energy spectrum. However, there is some controversy whether or not the statistics of presently existing data gives support to the model.

Recently, a more particle physics motivated picture of explaining the knee was put forward by Wigmans⁵. He suggested that inverse beta decay of protons with massive relic neutrinos according to $p + \bar{\nu}_e \rightarrow n + e^+$ could destroy protons. Simple kinematics shows that this channel is open for $E_p > 1.7 \cdot 10^{15} \text{ eV}/m_\nu(\text{eV})$. Thus, the knee energy $E_{\text{knee}} \simeq 4 \text{ PeV}$ would correspond to an electron neutrino mass of $\sim 0.4 \text{ eV}$, a value presently not excluded by any

other observation or experiment. However, ‘eating’ sufficiently large amounts of protons by such a process requires extraordinary high local densities of relic neutrinos, even if possible gravitational trapping is considered.

It has also been suggested that the knee is not a property of the primary energy spectrum itself, but rather may be caused by changing high-energy interactions in the earth atmosphere⁶. Producing a new type of a heavy particle in the first interactions escaping unseen by air shower experiments could, in principle, mimic a break in the spectrum. From the particle physics point of view this is not completely ruled out as the centre-of-mass energy available at the knee is above Tevatron energies. Different from the astrophysical interpretations of the knee, one would now expect to see the knee energy of different primary particles being displaced by their mass number A rather than by their charge Z . This is understood from the nuclear reaction mechanism being governed by the energy per nucleon E/A of the incident particle.

A key observable for understanding the origin of the knee and distinguishing the SN acceleration model from the other proposed mechanisms, is thus given by CR energy spectra of different elemental groups or, if measured more inclusively, by the mass composition of CRs measured across the knee (see e.g. Ref.²). This is to be complemented by measurements of anisotropies in the arrival directions of CRs. Finally, experiments should also aim at testing hadronic interaction models by means of air shower data.

At present, beyond the knee little is known about CRs other than their all-particle energy spectrum⁷. The low flux of particles ($\sim 1 \text{ m}^{-2}\cdot\text{year}^{-1}$ above the knee) puts strong demands on the collection power of the experiments, such as can at present only be achieved by extended air shower (EAS) arrays at ground level. The development of an EAS is a process of truly multi-particle dynamics with frequent high-energy hadronic and electromagnetic interactions taking place. At primary energies of 10^{15} eV about 10^6 particles reach sea-level. These are mostly photons and electrons plus some fraction of high-energy muons and hadrons, spread out over an area of several hectares. Sampling detector systems with typical coverages of less than one percent can thus be used for registration of such EAS. However, this indirect method of detection bears a number of serious difficulties in the interpretation of the data and requires detailed modelling of the air shower development (see talk given by D. Heck⁸) and detector responses. Particularly, systematic effects caused by the employed high-energy interaction models and by inevitable EAS fluctuations need to be considered. The basic concept of the KASCADE experiment is to measure a large number of EAS parameters in each individual event in order to verify the consistency of EAS simulations and to determine the energy and mass of the primary particles on a reliable basis. It is hoped

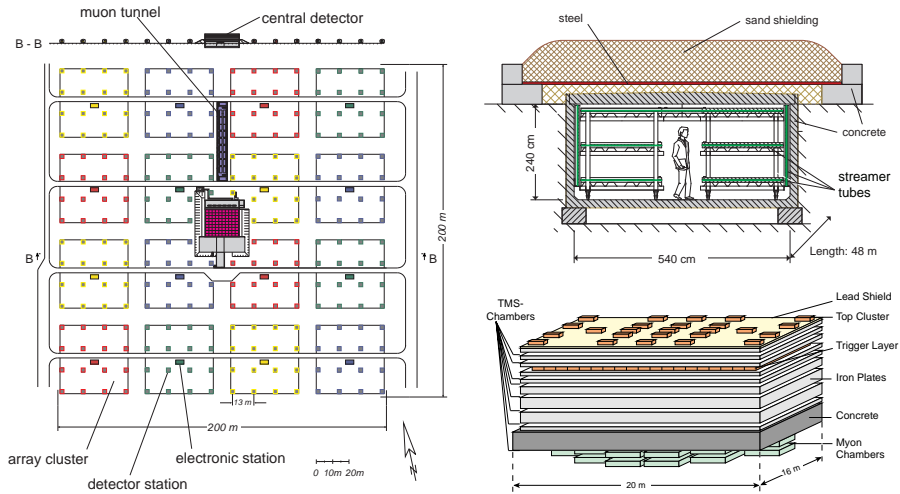


Figure 1. Schematic layout of the KASCADE experiment (left), with its streamer tube tracking system (top right) and central detector (bottom right)⁹.

that the new data will substantially improve our knowledge of the origin of high-energy cosmic rays.

2 KASCADE Experiment

KASCADE (Karlsruhe Shower Core and Array Detector) is located at the laboratory site of Forschungszentrum Karlsruhe, Germany (at 8° E, 49° N, 110 m a.s.l.). In brief, it consists of three major components (see Fig. 1);

1. A scintillator array comprising 252 detector stations of electron and muon counters arranged on a grid of $200 \times 200 \text{ m}^2$ and providing in total about 500 m^2 of e/γ - and 620 m^2 of μ -detector coverage. The detection thresholds for vertical incidence are $E_e > 5 \text{ MeV}$ and $E_\mu > 230 \text{ MeV}$.
2. A central detector system (320 m^2) consisting of a highly-segmented hadronic calorimeter read out by 40,000 channels of warm liquid ionization chambers, a layer of scintillation counters above the shielding, a trigger plane of scintillation counters in the third layer and, at the very bottom, 2 layers of positional sensitive MWPC's, and a streamer tube layer with pad read-out for muon tracking at $E_\mu \geq 2.4 \text{ GeV}$.

3. A $48 \times 5.4 \text{ m}^2$ tunnel housing three horizontal and a two vertical layers of positional sensitive limited streamer tubes for muon tracking at $E_\mu \geq 0.8 \text{ GeV}$.

More details about the experiment can be found in Refs. ^{9,10}. First correlated data have been taken with some parts of the experiment in 1996 and with its full set-up since 2000. At present, more than 300 Mio. events have been collected in a very stable mode and with a trigger threshold of the array corresponding to $E \sim 4 \cdot 10^{14} \text{ eV}$.

3 Tests of High-Energy Hadronic Interaction Models

The observation of EAS provides an opportunity to study global properties of hadronic interactions in an energy range not accessible to man-made accelerators. For example, the centre-of-mass energy at the Tevatron collider corresponds to a fixed target energy in the nucleon-nucleon system of $E_p \simeq 1.7 \cdot 10^{15} \text{ eV}$. Even more importantly, the diffractive particle production dominating the energy flux in the forward region and influencing the EAS development most strongly, was studied experimentally only at comparatively low energies of $\sqrt{s} \simeq 10 \text{ GeV}$ ¹¹. Most of the beam energy in present collider experiments, however, remains unseen. For example, the UA5 experiment could register up to 30% of the total collision energy at $\sqrt{s} = 0.9 \text{ TeV}$, while the CDF detector registers only about 5% at $\sqrt{s} = 1.8 \text{ TeV}$. Hence, hadronic interaction models applied to higher energies and to particle production in the forward region rely on extrapolations and may cause systematic uncertainties in simulations of EAS. Additional uncertainties arise from simulations of p-nucleus and nucleus-nucleus collisions including a possible formation of a quark-gluon plasma. Again, such data are important for EAS interpretations but have been studied only at low energies in the past (SPS and ISR at CERN). Only very recently, RHIC data at $\sqrt{s} = 200 \text{ GeV}$ have become available and will be very helpful in this respect. Apart from different theoretical extrapolations, an additional source of uncertainty for all models originates from the experimentally deduced energy dependent inelastic cross-sections¹². At Tevatron energies, the proton-antiproton cross section is not known to better than 5% at best. As will be shown below, these uncertainties are amplified when predicting absolute hadron fluxes at sea-level by means of EAS simulations. Thus, one may take advantage of this strong dependence and perform stringent tests of models on the basis of EAS data. The idea is to use data of *absolute* CR fluxes up to several TeV of energy, as obtained from balloon and satellite experiments at the top of the atmosphere,

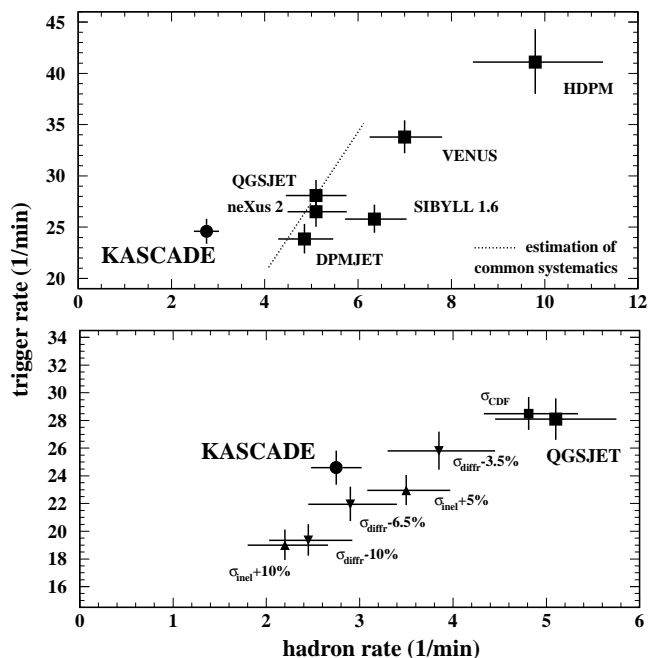


Figure 2. Trigger rate vs hadron rate in KASCADE. The top panel compares different hadronic interaction models to the experimental data. The systematic uncertainty, mostly given by the absolute flux uncertainty of the direct experiments, is indicated by the dotted line. The lower panel shows results obtained from the QGSJET¹⁶ model with modified inelastic cross section and diffraction dissociation^{14,15}.

and propagate these particles (taking into account their energy distribution and chemical composition) through the atmosphere employing the CORSIKA simulation package¹³. At the level of the KASCADE experiment, we then ask for triggers released by either high energy hadrons ($E_h > 90$ GeV) or a minimum number of 9 muons detected in the central detector of KASCADE. These simulated inclusive trigger rates, employing different hadronic interaction models, are then compared to actual experimental data^{14,15}. Figure 2 shows the results. None of the predictions agrees well with the experimental data, particularly the hadron rates are overestimated by up to a factor of 3. Furthermore, there are also large differences found between the models. This convincingly proves the sensitivity of the experimental observable to details of the interaction models.

Earlier investigations of high-energy hadrons observed in the shower core

of the KASCADE calorimeter¹⁷ lead to the conclusion that QGSJET provides the best overall prescription of EAS data. This was confirmed also by an independent analysis including data from different EAS experiments¹⁸. Therefore, several modifications were applied to the QGSJET model in order to study their influence to the predicted trigger rates. Results are presented in the lower panel of Fig. 2. Increasing the inelastic proton-air cross section by 5 and 10 % reduces the predicted hadron rate by approx. 27 % and 54 %, respectively. Similar effects are obtained by lowering the diffraction dissociation by up to 10 % of the inelastic cross section. Clearly, there is a strong sensitivity to these parameters. Since the total inelastic cross section appears to be the better known quantity, we conclude that the diffraction dissociation is overestimated in the simulated hadron-nucleus interactions by about 5 % of the inelastic cross section $\sigma_{\text{inel}}(\text{p-air})$. Further studies with new models and with high energy hadrons observed in the core of EAS are in progress and will, hopefully, help to further improve our understanding of hadronic interaction processes in EAS. This will be important also for interpretations of EAS data in terms of primary energy and chemical composition.

4 Energy Spectrum and Chemical Composition

Extracting the primary energy and mass from EAS data is not straightforward and a model must be adopted to relate the experimental observables to properties of the primary particle. As shall be discussed below, the analysis is complicated by large fluctuations of EAS observables and by the fact, that virtually all of these observables are sensitive to changes in the mass *and* energy of the primary particle.

Air shower measurements generally include particle measurements at ground and are sometimes complemented by detection of Cherenkov- and fluorescence light¹⁹. Primary observables of KASCADE are lateral particle density distributions, $\rho_{e,\mu,h}(r)$, and their integrals $N_{e,\mu,h} = \int_{r_1}^{r_2} 2\pi r \rho_{e,\mu,h}(r) dr$, yielding total (if extrapolations $r_1 \rightarrow 0$ and $r_2 \rightarrow \infty$ are made) or truncated particle shower sizes. Truncated shower-sizes, $N_{e,\mu,h}^{\text{tr}}$, have been introduced by the KASCADE collaboration in order to avoid systematic uncertainties resulting from extrapolations of $\rho_{e,\mu,h}(r)$ to large distances not covered by the experiment. Reconstruction techniques of the individual particle densities, shower core position, and shower direction have been discussed in Ref. ²⁰. As simulations predict and as it is obvious from very basic considerations, the weighted sum of particle shower sizes provides an estimate of the primary energy, i.e. $E \simeq a \cdot \log N_{\mu}^{\text{tr}} + b \cdot \log N_e^{\text{tr}}$, with a and b determined from simulations. On the other hand, the ratio $Y_{\text{ratio}} = \log N_{\mu}^{\text{tr}} / \log N_e^{\text{tr}}$ provides a

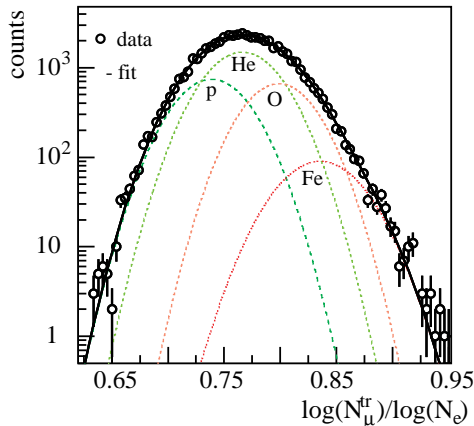


Figure 3. Example of an event-by-event distribution of the muon/electron ratio measured by KASCADE for a primary energy of $E \simeq 3 \cdot 10^{15}$ eV. The lines show results of CORSIKA simulations employing the QGSJET model and are performed for different primary particles.

reliable estimate of the primary mass²¹. This is mostly because showers of heavy primaries will, on average, develop higher in the atmosphere so that the electromagnetic component suffers more absorption in the atmosphere as compared to a shower induced by a primary proton¹⁹. An example is presented in Fig. 3. Clearly, a superposition of different particle types (represented by the lines) is required to account for the experimental distribution. Noteworthy, the left and right hand tails of the experimental distribution are nicely described by the proton and iron simulations, respectively. Performing such an analysis for different bins of shower sizes

yields an increasingly heavier composition for energies above the knee²¹.

The separation of primary particle types by Y_{ratio} may also be used to disentangle the primary flux spectrum into ‘light’ and ‘heavy’ components. An example is shown in Fig. 4. Here, the distribution of muon densities measured in the trigger plane of the central detector at a distance of 45.5 m from the shower core is plotted for all showers and for those where $Y_{\text{ratio}} < 0.75$ (‘electron-rich’) and $Y_{\text{ratio}} > 0.75$ (‘electron-poor’). Interestingly, the knee structure is seen for unselected and electron-rich showers but is absent for electron-poor showers^{22,23}. Realizing that the muon density at given distance to the shower core is linked to the primary energy, the figure proves in a very model independent way that *the knee structure appears to be a feature caused by the light component only*. Again, we like to stress that ρ_{μ} is directly measured by the experiment and that any meaningful model will predict electron-rich and -poor showers for light and heavy primaries, respectively.

This finding is confirmed by combined energy and composition analyses of the shower size spectra of KASCADE, albeit then based on quantitative Monte Carlo simulations. A compilation of the all-particle energy spectrum reconstructed from various experiments is presented in figure 5. The agreement appears reasonable and deviations are mostly explained by uncertainties in the energy scale by up to 25%, e.g. CASA MIA data²⁴ were shifted up-

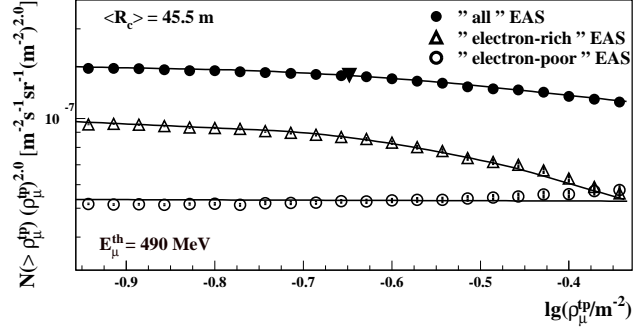


Figure 4. Distribution of muon densities ρ_μ ($E_\mu > 490$ MeV) measured in the trigger plane at a distance of 45.5 m from the shower axis. The ‘all’-particle spectrum is shown as well as spectra for ‘electron-rich’ and ‘-poor’ showers. The black triangle indicates the position of the knee^{22,23}.

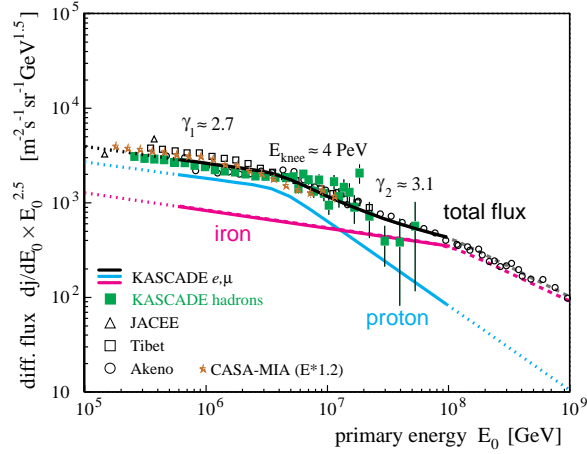


Figure 5. Primary energy spectrum as obtained from different experiments. The lines represent KASCADE results based on a simultaneous fit to electron and muon shower sizes assuming the all-particle spectrum to be a superposition of a proton and iron component²⁶.

wards in energy by 20% to yield a better agreement to the other data sets. The shift is likely to be explained by the interaction model SIBYLL 1.6²⁵ employed by the authors of Ref. ²⁴ but which has been proven to provide only a poor description of the experimental data¹⁷. The lines correspond to a simultaneous fit of the electron and muon size spectra of KASCADE, assuming the

all-particle spectrum to be described by a sum of proton and iron primaries²⁶. Energy and mass dependent fluctuations of the electron and muon shower size are taken into account in this analysis and, in fact, turn out to be important for any quantitative discussion. Again, the knee is only reconstructed for the light component and no indication of a break is seen in the heavy component up to about 10^{17} eV. Obviously, the different spectral shapes of the ‘light’ and ‘heavy’ induced air showers will result in an increasingly heavier composition above the knee, such as is found also by other experiments. The analysis is an ongoing process with improved statistics and reconstruction techniques making use of the multi-detector capabilities of KASCADE.²⁷

5 Conclusions and Outlook

KASCADE data provide mounting evidence for the knee being caused by the light particle component only. Up to an energy of $\sim 10^{17}$ eV, which is the upper limit of the present KASCADE experiment, no indication of a similar structure is found in the iron-like distribution. However, comparison to the all-particle spectrum deduced from other experiments, suggests the necessity of a similar break in the heavy component just above 10^{17} eV. This important finding gives direct support to the picture of acceleration or galactic confinement in magnetic fields. To discriminate the two pictures, high statistics data on anisotropy will be required and are currently being analysed. Furthermore, an extension of the mass-selective measurements to higher energies appears mandatory in order to test the hypothesis of a ‘Fe-knee’ in more detail. This should go in parallel with further tests of hadronic interaction models in order to improve the reliability of the EAS data analysis.

The KASCADE and EAS-TOP²⁸ collaborations have just started a common effort to realise these goals already in the near future. The EAS-TOP scintillators are currently positioned next to the KASCADE experiment at the site of Forschungszentrum Karlsruhe providing a 12 times larger acceptance as compared to the present set-up. Generating a common trigger for the combined experimental installations will allow taking advantage of the full multi-detector capabilities including hadronic measurements as well as muon counting, tracking, and timing capabilities. The new installation is foreseen to start taking data in spring 2002. It is expected that the upcoming KASCADE and future KASCADE-GRANDE data will allow extending the tests of hadronic interaction models to higher energies and to substantially improve our understanding of the origin of the knee in particular and about the origin and acceleration of cosmic rays in general.

References

1. L. O'C. Drury, *Contemp. Phys.* **35** (1994) 231
2. E.G. Berezhko, L.T. Ksenofontov, *J. Exp. Theor. Phys.* **89** (1999) 391
3. T.K. Gaisser, preprint astro-ph/0011524, 2000
4. A.D. Erlykin and A.W. Wolfendale, *J. Phys.* **G23** (1997) 979
5. R. Wigmans, *Nucl. Phys. B (Proc. Suppl.)* **85** (2000) 305
6. S.I. Nikolsky, *Nucl. Phys. B (Proc. Suppl.)* **39A** (1995) 228
7. A.A. Watson, *25th ICRC Durban* **8** (1998) 257
8. D. Heck et al., *Proc. XXX Int. Symp. Multipart. Dynamics*, eds. T. Csörgő et al., (World Scientific, Singapore) 2001
9. H.O. Klages et al., *Nucl. Phys. (Proc. Suppl.)* **52B** (1997) 92
10. P. Doll et al., Report KfK 4648, Kernforschungszentrum Karlsruhe, 1990
11. A.B. Kaidalov, *Phys. Rep.* **50** (1979) 157
12. T. Stanev, M.M. Block, F. Halzen, *Phys. Rev.* **D62** (2000) 077501
13. D. Heck et al., Report FZKA 6019, Forschungszentrum Karlsruhe, 1998
14. M. Risse et al., *26th ICRC Salt Lake City* **1** (1999) 135.
15. T. Antoni et al., "*Test of Hadronic Interaction Models in the Forward Region with KASCADE Event Rates*", submitted to *J. Phys.* **G** (2001)
16. N.N. Kalmykov and S.S. Ostapchenko, *Yad. Fiz.* **56** (1993) 105
17. T. Antoni et al., *J. Phys.* **G25** (1999) 2161
18. A.D. Erlykin and A.W. Wolfendale, *Astropart. Phys.* **9** (1998) 213
19. K.-H. Kampert, (preprint astro-ph/0101283), *J. Phys.* **G** (2001), in press
20. T. Antoni et al., *Astropart. Phys.* **14** (2001) 245
21. T. Antoni et al., *Nucl. Phys. (Proc. Suppl.)* **75A** (1999) 234
22. T. Antoni et al., "*Muon density measurements with the KASCADE Central Detector*", subm. to *Astropart. Phys.* (2001)
23. A. Haungs et al., *26th ICRC Salt Lake City* **1** (1999) 218
24. M.A.K. Glasmacher et al., *Astropart. Phys.* **10** (1999) 291
25. R.S. Fletcher, et al., *Phys. Rev.* **D50** (1994) 5710.
26. R. Glasstetter et al., *26th ICRC Salt Lake City* **1** (1999) 222
27. T. Antoni et al., "*A non-parametric approach to infer the energy spectrum and mass composition of cosmic rays*", *Astropart. Phys.* (2001), in press
28. M. Aglietta et al., *Nucl. Instr. Meth.*, **A277** (1989) 23